Evaluation of Tsunami Risk Posed to Sri Lanka by Potential Mega-Thrust Earthquakes in the Makran Subduction Zone

J J Wijetunge

Abstract: This paper is concerned with a numerical study carried out to assess the threat posed to Sri Lanka by potential tsunamigenic earthquakes in the Makran subduction zone in the Arabian Sea off the south coasts of Pakistan and Iran. The fault plane model adopted in the present simulations corresponds to a worst-case scenario of simultaneous rupture of the entire eastern segment of the Makran Trench. A hydrodynamic model based on linear shallow-water equations was employed to simulate tsunami propagation from the source to the shoreline around Sri Lanka. The numerical simulations suggest that the maximum nearshore tsunami amplitudes along the coastal belts of the Western, North-Western and Southern Provinces are of the order of 1 m; the corresponding values for the Eastern and Northern provinces are even smaller, about 0.2 m and 0.1 m, respectively. The model results also indicate that the tsunami waves will first hit the coastal belt of the Western Province about 280 minutes after the earthquake, followed by Southern and North-Western Provinces. The results presented in this paper would be useful for authorities responsible for evacuation to make a better judgement as to the level of threat in different areas along the coastline, and to act accordingly, if a large earthquake were to occur in the Makran subduction zone.

Keywords: Tsunami Amplitude, Makran Subduction Zone, Risk Assessment, Shallow-Water Equations, Numerical Modelling

1. Introduction

The earthquake of moment magnitude M_w=9.1-9.3 [9] on 26 December 2004 in the Andaman-Sunda trench ruptured a 1200 km long segment, starting near the northern part of the Sumatra Island and ending offshore of the Andaman Islands. The impact on Sri Lanka of the tsunami unleashed by the 2004 earthquake has already been examined in detail (for example, Dias *et al.* [4], Fernando *et al.* [5], Hettiarachchi and Samarawickrama [7], Illangasekera *et al.* [8], Rossetto *et al.* [16], Tomita *et al.* [17], Wijetunge [19], Wijetunge *et al.* [21]). Two subsequent major earthquakes on 25 March 2005 (M_w=8.6) and on 12 September 2007 (M_w=8.5) in the Sunda trench further south of the 2004 event produced only comparatively smaller tsunamis in the far-field. Among other reasons, the location and the orientation of the fault planes of these two earthquakes were such that the bulk of the tsunami energy was directed away from Sri Lanka.

Besides the Andaman-Sunda Trench which produced the massive 2004 tsunami, the potential for occurrence of large tsunamigenic earthquakes that could affect Sri Lanka exists at two other subduction zones, namely, the Arakan Trench off Myanmar in the northern Bay of Bengal and the Makran Trench off Pakistan and Iran in the Arabian Sea [10] (See Fig. 1 for locations of these seismic zones).

As for the seismogenic potential of the fault line further north of Andaman Islands, Cummins [2] concluded that the Arakan Trench located off Myanmar is capable of generating a giant tsunamigenic earthquake with potential for causing great loss of lives and destruction. His assessment was based on a detailed examination of the tectonic environment, stress and crustal strain observations as well as historical earthquake activity in the Arakan subduction zone. Wijetunge [20] examined the level of hazard posed to Sri Lanka by such a tsunami originating in the Arakan Trench by computing the likely maximum wave heights along the shoreline of the island. His numerical simulations indicated that, in Sri Lanka, the Northern Province would be at a greater risk from a tsunami generated in the Arakan fault plane with maximum nearshore wave amplitudes on the order of 10 m, whilst the

Eng. (Dr) J. J. Wijetunge, AMIE (Sri Lanka), BSc Eng (Hons) (Moratuwa), PhD (Cambridge), Senior Lecturer (Coastal & Ocean Engineering), Department of Civil Engineering, University of Peradeniya.

ENGINEER
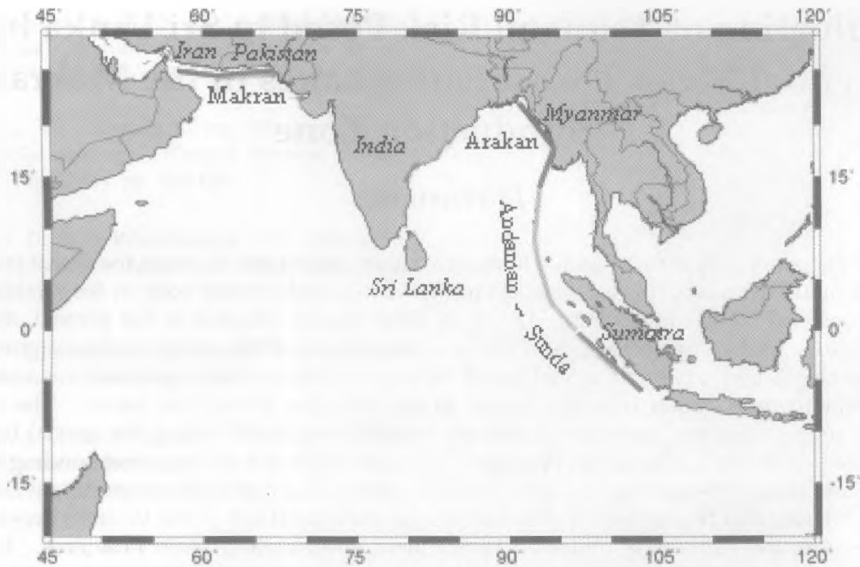
Figure 1 - Active Subduction Zones Around Sri Lanka: Makran, Arakan, and Andaman and Sunda Trenches.

maximum amplitudes along the Eastern and Southern Provinces could reach up to about 5.6 m and 2.6 m, respectively. On the other hand, Western Province in the shadow of direct tsunami impact would only receive small waves of amplitude up to 0.6 m.

However, unfortunately, little is known about the order of magnitude of likely tsunami heights along the coastal belt of Sri Lanka from a potential mega-thrust earthquake in the Makran Trench off Pakistan. Accordingly, in this paper, a numerical model of tsunami propagation is employed to evaluate the level of risk to Sri Lanka from a tsunami generated by a potential mega-thrust earthquake in the Makran Trench.

2. Tectonic Setting

The Makran region of southern Pakistan and south-eastern Iran is a 1000 km section of the Eurasian-Arabian plate boundary, where the Arabian plate sinks under the Eurasian plate (Fig. 2). The convergence rate of the Arabian and Eurasian plates along the Makran fault is estimated at 36.5 mm/yr to 42.0 mm/yr [3].

A number of presumably large historical earthquakes have been documented along the Makran coast. Byrne *et al*. [1] noted that the Makran subduction zone exhibits a strong segmentation between east and west in its seismic behavior. This is because the plate boundary in eastern Makran ruptures in large

and great thrust earthquakes, whilst in contrast, western Makran exhibits no well-documented great earthquakes in historic times, and modern instrumentation has not detected any shallow events along the plate boundary. On the eastern segment of Makran, the three blocks labelled 'A', 'B' and 'C' in Fig. 2 identify the probable rupture areas of three great earthquakes that occurred in 1851, 1945 and 1765. The 28 November 1945 (M_w=8.0) earthquake generated the most recent major tsunami in the Arabian Sea. More than 4000 people were killed on the Makran coast by both the earthquake and the tsunami. The run-up in Makran was 17 m and at Kutch in north-western India 11 m. Further south on the west coast of India, this tsunami caused damage in Mumbai with 2 m run-up and affected Karnataka too [10], [13]. On the other hand, the only known earthquake that may potentially have struck western Makran is that reported to have caused damage in the Strait of Hormuz and north-east Oman in 1483. However, determination of a more specific location for this earthquake is not possible due to paucity of information. [1]

Subsequent to a review of the tectonic setting and the seismic history of the Makran subduction zone, Okal and Synolakis [15] proposed a 'worst-case' tsunamigenic earthquake scenario involving the simultaneous rupture of the 1851 ('A'), 1945 ('B') and 1765 ('C') fault zones, shown in Fig. 2. The fault parameters corresponding to this scenario, which have been adopted in the present study,

are given in Table 1. Moreover, Okada's [14] dislocation model is used to obtain the initial sea surface elevation (see Fig. 3) for the above co-seismic tsunami source, assuming that the sea surface follows the sea bed deformation instantaneously.
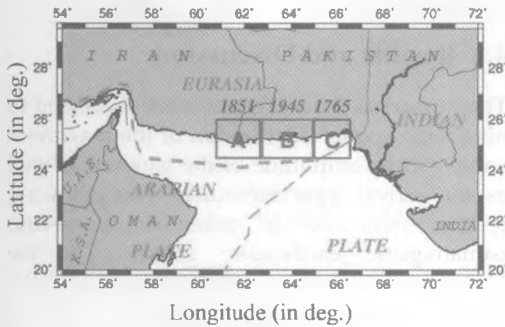
Figure 2 – Map of the Makran coast of Pakistan and Iran. The Three Blocks Labelled 'A', 'B' and 'C' Identify the Probable Rupture Areas of the Earthquakes of 1851, 1945 and 1765. (Modified After Byrne *et al.*, [1]).

Table - 1 Fault Parameters Adopted in the Present Study.

Parameter	Value
Coordinates of centroid (x_0, y_0)	(64.0°E, 25.3°N)
Length, L	550 km
Width, W	100 km
Dip, δ	7 deg.
Rake, λ	89 deg.
Strike, φ	265 deg.
Depth, d	15 km
Slip, Δ	7 m

3. Numerical Modelling

In the following, the system of nested grids adopted and the hydrodynamic model employed to simulate the propagation of a tsunami that could be caused by a mega-thrust earthquake in the Arakan subduction zone are outlined.

3.1 Grid Set-Up

A dynamically coupled system of two nested grids was employed to simulate the tsunami propagation from Makran subduction zone towards the shoreline of Sri Lanka. The bathymetry data for the largest grid employed in the simulations, i.e., Grid-1 shown in Fig. 4, was obtained by interpolating GEBCO data with a resolution of 1 arc-minute to a grid of 1.3560 arc-minutes (~ 2500 m) spacing. Grid-2, which is embedded in Grid-1 for the simulation

of tsunami propagation over the shallow continental shelf off Sri Lanka at a finer resolution of 0.2712 arc minutes (~ 500 m), is also shown in Fig. 4.
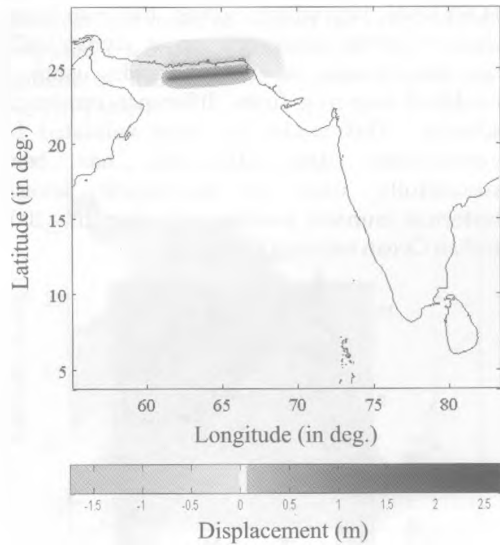
Figure 3 - The Initial Sea-Surface Displacement from the Fault Model.
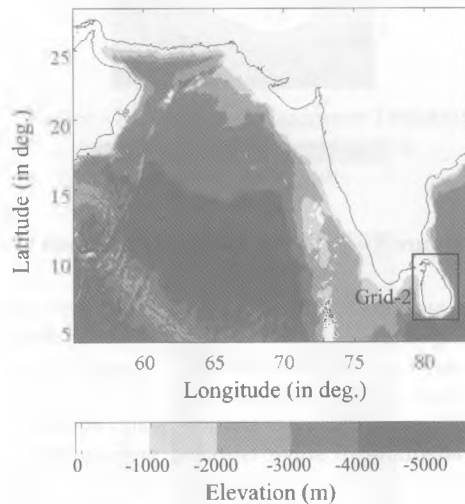
Figure 4 – Grid-1 of the Computational Domain; Location of Grid-2 is Also Shown.

The bathymetry for Grid-2 shown in Fig. 5 was at first interpolated from GEBCO grid and was then updated with data from navigation charts. These navigation charts typically covered depths down to about 3000 m–4000 m at scales of 1:150,000 or 1:300,000. The nearshore bathymetry at some localities was further updated with data from higher resolution navigation charts at scales of 1:10,000 and 1:15,000.

ENGINEER

3.2 Model Formulation

The mathematical model used in the present work is the Cornell Multi-grid Coupled Tsunami Model (COMCOT, coded in FORTRAN 90) which solves the non-linear shallow water equations on a dynamically coupled system of nested grids using a modified leap-frog finite difference numerical scheme. This model has been validated by experimental data [11] and has been successfully used to investigate several historical tsunami events, including the 2004 Indian Ocean tsunami ([18], [21]).

Figure 5 – Grid-2 of the Computational Domain.

The amplitude of a trans-oceanic tsunami during its propagation is typically in the order of magnitude of 1 m, whilst the wavelength of the leading wave is in the order of magnitude of 100 km. Thus, linear shallow water equations are adequate to solve tsunami propagation in Grids-1 and -2. Furthermore, as the spatial extent is comparatively larger in Grids-1 and -2, the spherical coordinate system is used to solve the set of linear shallow water equations given in the following:

$$\frac{\partial \zeta}{\partial t} + \frac{1}{R \cos \varphi} \left| \frac{\partial P}{\partial \psi} + \frac{\partial}{\partial \varphi} (\cos \varphi Q) \right| = 0$$

$$\frac{\partial P}{\partial t} + \frac{gh}{R \cos \varphi} \frac{\partial \zeta}{\partial \psi} - fQ = 0 \qquad \cdots\cdots (1)$$

$$\frac{\partial Q}{\partial t} + \frac{gh}{R} \frac{\partial \zeta}{\partial \varphi} + fP = 0$$

where, ζ is free surface elevation; ψ and φ denote the longitude and latitude of the Earth,

respectively; R is the Earth's radius; P and Q stand for the volume fluxes ($P = hu$ and $Q = hv$, with u and v being the depth-averaged velocities in longitudinal and latitudinal directions, respectively); h is the still water depth; and f represents the Coriolis force coefficient.

4. Results and Discussion

The numerical model results were processed to obtain the spatial distribution of the maximum values of the amplitude of the tsunami as well as the arrival time contours. The following results refer to a potential worst-case tsunamigenic earthquake scenario in the Makran subduction zone corresponding to the fault parameters given in Section 2.

First, Fig. 6 shows three snapshots of the simulated tsunami wave front approaching Sri Lanka at: (a) $t = 1$ hr, (b) $t = 2$ hrs, and (c) $t = 4$ hrs after the earthquake. We see that, in the far-field, the west coast of India, the Maldive Islands, and to a lesser degree, the west and south coasts of Sri Lanka are exposed to the tsunami wave front, besides the south coasts of Pakistan and Iran as well as Oman in the neighbourhood of the fault plane. However, the geographical location of the fault plane ensures that the entire east coast and a part of the north coast of Sri Lanka as well as the east coast of India are in the shadow of direct impact of tsunami waves.

Now, Figs. 7 and 8, respectively, show shaded plots of the spatial variation of the maximum values of the computed tsunami amplitudes across the Arabian Sea and around the continental shelf off Sri Lanka.

Fig. 7 indicates that the orientation of the fault line is such that, in the far-field, the maximum energy is directed in a south-easterly direction towards the Maldive Islands. It also appears that, although located lateral to the maximum energy zone, certain stretches of the west coast of India too could be hit by significantly larger wave heights owing to the effects of shoaling and energy focusing caused by the bathymetry. However, it is not intended to examine the nearshore tsunami amplitudes along the east coast of India in detail in the present analysis. This is because model results for the shoreline off the east coast of India are available only from Grid-1 with a coarser spatial resolution; moreover, the bathymetry off India is based only on those of 1 arc-minute resolution and

has not been updated with data from higher resolution navigation charts.
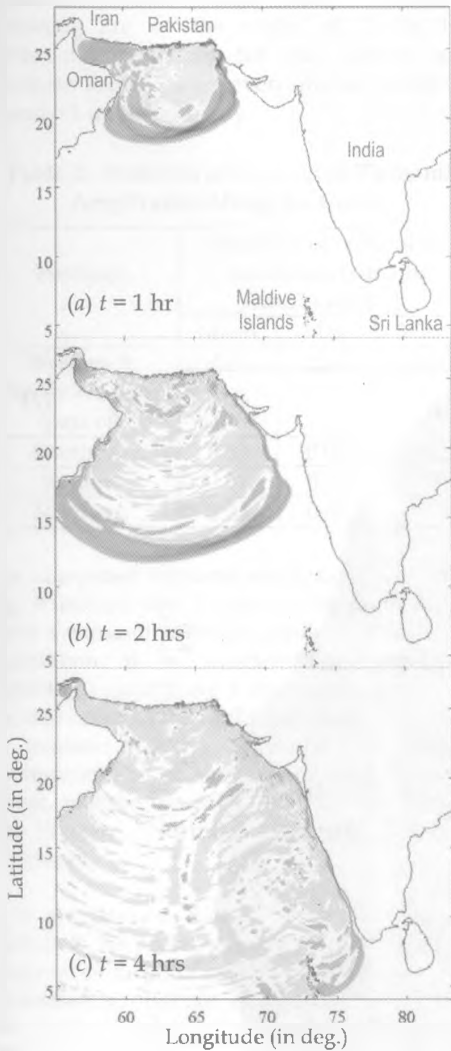
Figure 6 - Snapshots of Tsunami Wave Front Approaching the Coastline of Sri Lanka at: (a) t = 1 hr, (b) t = 2 hrs, and (c) t = 4 hrs After the Earthquake.

Fig. 8 indicates that the maximum tsunami amplitudes, although lower than about 1 m, are relatively larger around the west and the north-west coasts, moderate along the south coast, and smaller around most of the east and north coasts.

Now, in order to have a closer look at the peak water levels expected along the coastal belt, we consider the maximum tsunami amplitudes extracted from Grid-2 at water points nearest to the shoreline at a mean water depth of 3.6 m. Accordingly, Fig. 9 shows the variation of the

maximum tsunami amplitude with longitude (°E) or latitude (°N) of the coastline along: (a) Western Province and part of North-Werstern Province, (b) Southern Province, (c) Eastern Province, and (d) Northern Province. Moreover, the mean as well as the range of the computed tsunami amplitudes for each segment of the coast at provincial level are given in Table 2.
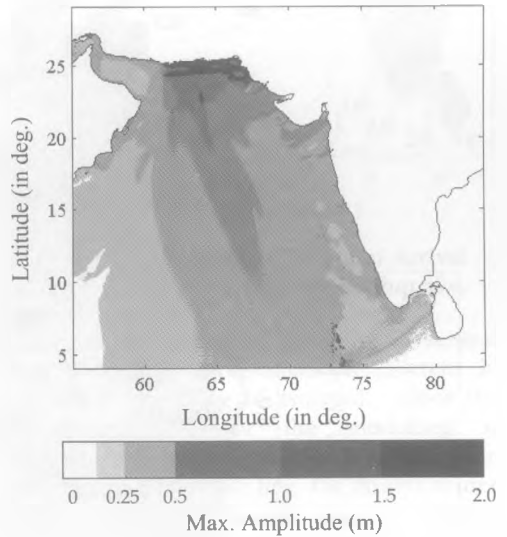
Figure - 7 Computed Maximum Tsunami Amplitude Across Arabian Sea.
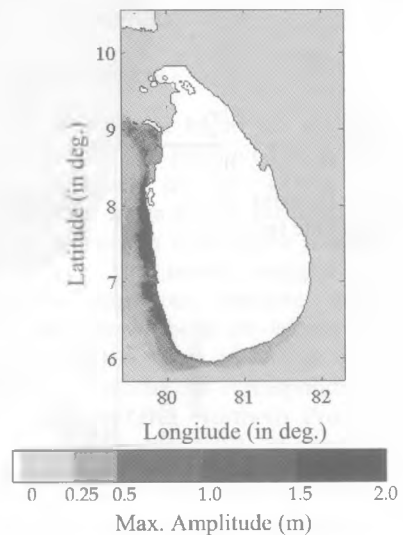
Figure 8 - Computed Maximum Tsunami Amplitudes Around Sri Lanka.
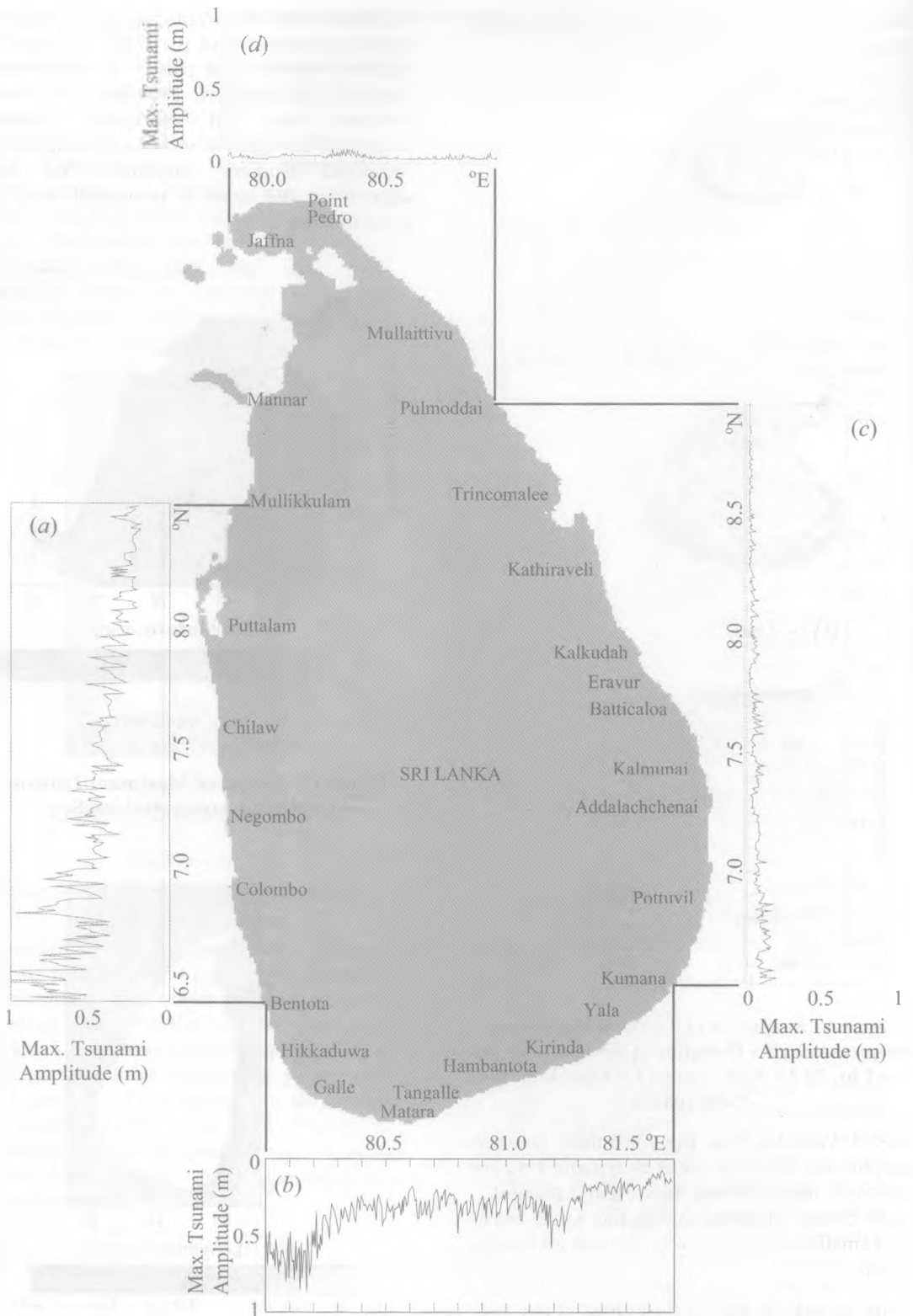
Figure 9 - Computed Maximum Tsunami Amplitudes at Water Points Nearest to the Shoreline: (*a*) Western Province and Part of North-Werstern Province, (*b*) Southern Province, (*c*) Eastern Province, and (*d*) Northern Province.

Table 2 indicates that the maximum nearshore tsunami amplitudes along the coastal belts of Western, North-Western and Southern Provinces are of the order of 1 m; the corresponding values for the Eastern and Northern Provinces are even smaller, about 0.2 m and 0.1 m, respectively.

Table 2 - Statistics of Computed Tsunami Amplitudes Along the Coast.

Province	Statistics of computed maximum tsunami amplitude (m)		
	Mean	Min.	Max.
Western & North-Western (part of)	0.41	0.14	1.15
Southern	0.33	0.08	0.87
Eastern	0.07	0.03	0.21
Northern	0.04	0.03	0.09

The computed tsunami amplitudes shown in Fig. 9 indicate that it may not be necessary to issue a tsunami warning requiring immediate evacuation if a mega-thrust earthquake capable of generating a transoceanic tsunami were to occur in the Makran trench. However, a 'tsunami watch', requiring the coastal communities to be alert to a possible tsunami threat, may be issued to coastal areas only in the Western, North-Western and Southern Provinces.

It is emphasised that the numerical results such as those presented in Fig. 9 only give the likely amplitudes of oncoming tsunami waves immediately offshore of the coastline whilst the final run-up heights could be larger. Moreover, factors such as the onshore topography, the population density and the construction standards could further enhance or reduce the vulnerability of a given community.

Furthermore, the computed tsunami arrival time contours shown in Fig. 10 indicate that the tsunami waves will first hit the shoreline of the Western Province about 280 minutes after the earthquake, followed by Southern and North-Western Provinces.

The information presented in this paper relating to likely tsunami amplitudes and arrival times around the country would help authorities responsible for evacuation to make a better judgement as to the level of threat in different areas along the coastline, and to act

accordingly, if a large earthquake were to occur in the Makran subduction zone.
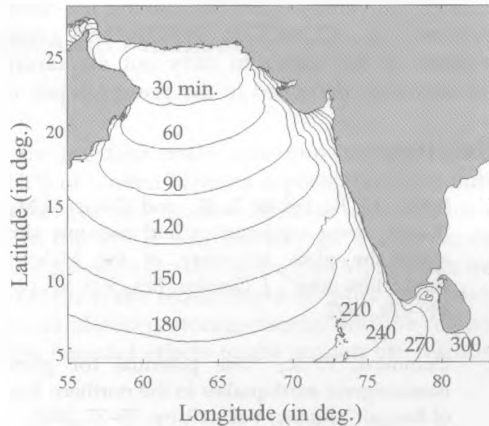
Figure 10 - Contours of Tsunami Arrival Times in Minutes After the Earthquake.

Finally, it must be added that there are several limitations and approximations inherent in numerical modelling of tsunami. Since the initial condition for the modelling is determined by the displacement of the ocean bottom along the fault line, the largest source of errors is the earthquake model. Another significant limitation is that the resolution of the modelling is no greater or more accurate than the bathymetric data used. Moreover, shallow water models such as that employed in the present study assume a uniform velocity profile across the flow depth and neglect vertical accelerations.

5. Conclusions

A numerical model based on shallow-water equations has been employed to evaluate the potential threat to Sri Lanka from a tsunamigenic mega-thrust earthquake in the Makran subduction zone off the south-coast of Pakistan. The results suggest that the maximum nearshore tsunami amplitudes along the coastal belts of Western, North-Western and Southern provinces are of the order of 1 m whilst the corresponding values for the Eastern and Northern Provinces are even smaller, about 0.2 m and 0.1 m, respectively.

The model results also indicate that the tsunami waves will first hit the Western Province about 280 minutes after the earthquake, followed by Southern and North-Western Provinces.

ENGINEER

Acknowledgment

References

1. Byrne, D. E., Sykes, L. R., and Davis, D.M., "Great thrust earthquakes and aseismic slip along the plate boundary of the Makran subduction zone", *J. Geophys. Res.*, Vol. 97, pp. 449-478, 1992.

2. Cummins, P. R., "The potential for giant tsunamigenic earthquakes in the northern Bay of Bengal.", *Nature*, Vol. 449, pp. 75–77, 2007.

3. DeMets, C., Gordon, R. G., Argus, D. F., and Stein, S., "Current plate motions", *Geophys. J. Int.*, Vol. 101, pp. 425–478, 1990.

4. Dias, P., Dissanayake, R. and Chandrathilake, R., "Lessons learned from tsunami damage in Sri Lanka, *Proceedings of ICE - Civil Engineering*, Vol. 159, pp. 74–81, 2006.

5. Fernando, P., Wikramanayake, E. D., and Pastorini, J., "Impact of tsunami on terrestrial ecosystems of Yala National Park, Sri Lanka", *Current Science*, Vol. 90 (11), 1531-1534, 2006.

6. GEBCO. *General Bathymetric Chart of the Oceans.* International Hydrographic Organization (IOC) of UNESCO. Available at: http://www.gebco.net/ (visited on 1-11-2008)

7. Hettiarachchi, S.S.L. and Samarawickrama, S.P., "Experience of the Indian Ocean Tsunami on the Sri Lankan coast", *Proc. of the Int. Symposium on Disaster Reduction on Coasts*, Melbourne, Australia, 2005.

8. Illangasekare, T., Tyler, S. W., Clement, P., Villholth, K. G., Perera, A. P. Obeysekera, J., Gunatilaka, A., Panabokke, C. R., "Impacts of the 2004 tsunami on groundwater resources in Sri Lanka", *Water Resources Research*, Vol. 42, W05201, 2006.

9. Ishii, M., P. M. Shearer, H. Houston, and J. E. Vidale., "Extent, duration and speed of the 2004 Sumatra–Andaman earthquake imaged by the Hi-Net array", *Nature*, Vol. 435, pp. 933-936, 2005.

10. Jaiswal, R. K., Rastogi, B. K., and Murty, T. S., "Tsunamigenic sources in the Indian Ocean", *Journal of Science of Tsunami Hazards*, Vol. 27, No. 2, pp. 32– 53, 2008.

11. Liu, Philip L.-F., Cho, Y.-S., Briggs, M. J., Synolakis, C.E., and Kanoglu, U., "Run-up of Solitary Waves on a Circular Island", *J. Fluid Mechanics*, Vol. 302, pp. 259-285, 1995.

12. Liu, P. L.-F., Lynett, P, Fernando, H, Jaffe, B. E., Fritz, H., Higman, B., Morton, R., Goff, J., and Synolakis, C. "Observations by the international tsunami survey team in Sri Lanka", *Science*, Vol. 308, 2005.

13. Murty, T. S., and and Rafiq, M., "A Tentative List of Tsunamis of the North Indian Ocean in the Marginal Seas", *Natural Hazards*, Vol. 4, pp. 81-83, 1991.

14. Okada, S., "Surface displacement due to shear and tensile faults in a half-space", *Bull. Seismol. Soc. Am.*, Vol. 75, pp. 1135–1154, 1985.

15. Okal, E. A., and Synolakis, C. E., "Far-field tsunami hazard from mega-thrust earthquakes in the Indian Ocean", *Geophys. J. Int.*, Vol. 172, pp. 995 - 1015, 2008.

16. Rossetto, T., Peiris, N., Pomonis, A., Wilkinson, S. M., Re, D. D., Koo, R. and Gallocher, S., "The Indian Ocean tsunami of December 26, 2004: observations in Sri Lanka and Thailand", *Nat. Hazards*, Vol. 42, No. 1, 2007.

17. Tomita, T., Imamura, F., Arikawa, T., Yasuda, T., and Kawata, Y., "Damage caused by 2004 Indian Ocean tsunami on the southwestern coast of Sri Lanka", *Coastal Engrg. Journal*, Vol. 48, No. 2, pp. 99-116, 2007.

18. Wang, X., and Liu, P. L. -F., "An analysis of 2004 Sumatra earthquake fault plane mechanisms and Indian Ocean tsunami", *Journal of Hydraulic Research*, Vol. 44, No. 2, pp. 147 – 154, 2006.

19. Wijetunge J. J., "Field measurements of the extent of inundation in Sri Lanka due to the Indian Ocean Tsunami of 26 December 2004". *Proc. of the Int. Symposium on Disaster Reduction on Coasts*, Melbourne, Australia, 2005.

20. Wijetunge, J. J., "Assessment of tsunami threat to Sri Lanka from potential mega-thrust earthquakes in the Arakan Subduction Zone", *J. Natn. Science Foundation of Sri Lanka*, 2008 (submitted for publication).

21. Wijetunge, J. J., Wang, X., and Liu, P. L. –F., "Indian Ocean Tsunami on 26 December 2004: Numerical modelling of inundation in three cities on the south coast of Sri Lanka". *Journal of Earthquake and Tsunami*, Vol. 2, No. 2, pp. 1–23, 2008.